Diffusional Boundary-Layer Resistance for Membranes with Low Porosity

DERMOT M. MALONE

and

JOHN L. ANDERSON

School of Chemical Engineering
Cornell University
Ithaca, New York 14853

Diffusional mass transfer across membranes with uniform but low pore densities was studied experimentally as a function of stirring rate and pore area fraction. The results were analyzed in terms of a stagnant film boundary-layer model specially formulated for a heterogeneous membrane containing discrete pores. The overall membrane diffusional resistance is linearly related to the inverse of the pore area fraction of the membranes for a constant stirring rate. An equivalent boundary-layer thickness can be defined which is independent of membrane properties but a unique function of stirrer speed. These experimental boundary-layer thicknesses are greater by a factor of 3 than those predicted by a published Sherwood number correlation determined for homogeneous surfaces, but the stirring rate dependence is in excellent agreement with this same correlation.

SCOPE

The correct interpretation or estimation of membrane transport rates requires a reasonably accurate description of boundary-layer effects operative at the membrane/fluid interfaces. For diffusional transport, the term unstirred layer is often used in referring to such effects. In complex situations, such as an internally stirred diaphragm diffusion cell, the fluid mechanics are poorly understood, and hence this description is often limited to a simple Sherwood number-Reynolds number correlation which, although proven for the experimental apparatus at hand, is not universally applicable to other cell designs. Colton and Smith (1972) have made what seems to be the first real attempt at correcting an experimental Sherwood number correlation for changes in certain design variables (impeller dimension, etc.) in a diaphragm cell.

Most boundary-layer Sherwood number correlations are obtained with the use of interfaces (membranes) which are homogeneous; that is, the total surface is available for solute transport. Some membranes, however, are heterogeneous with relatively few pores, such that the porosity (pore area or volume fraction) is quite low. The membrane surface contains discrete holes (pores) and diffusional flux lines near the surface must be distorted rather than being parallel, as for a homogeneous surface. Examples of low porosity membranes include those made by the track-etch process (for example, mica, Nuclepore®).

The questions addressed in this work are:

Can a stagnant film model (Keller and Stein, 1967) adequately describe boundary-layer effects on solute diffusion across low porosity (<5%) membranes?

Can the film thickness obtained from the diffusion data be related to existing correlations for boundary-layer mass transfer coefficients obtained with homogeneous membranes?

The experimental approach was to measure overall mass transfer coefficients for salt (potassium chloride) diffusion across well-defined membranes of variable but controlled porosity. The stirring rate of the bulk phases adjacent to the membrane was varied over the range 40 to 350 rev/min for each membrane. For any one stirring rate, the data were plotted as a function of membrane porosity in a manner designed to test the adequacy of the stagnant film model.

CONCLUSIONS AND SIGNIFICANCE

Our experimental results can be cast into a form which is consistent with a stagnant film model, where the film thickness (δ) is a function of the stirring rate but independent of the membrane porosity. If the boundary-layer mass transfer coefficient is calculated from $k_\infty = D_\infty/\delta$, where D_∞ is the solute diffusion coefficient, then the Sherwood number dependence on stirring Reynolds number agrees almost exactly with the correlation developed by Colton and Smith (1972) for benzoic acid dissolution in a diaphragm cell; however, the magnitudes of our Sherwood numbers are a factor of 3 lower than those predicted by their correlation. From our data alone, we cannot ascertain whether this discrepancy is the result of subtle differences in cell design (and impeller construction) or rather of a fundamental difference in convective-diffusion phenomena occurring at heterogeneous vs. homogeneous membrane/fluid interfaces.

The accurate estimation of rates of mass transfer between two phases has been the subject of a substantial portion of the chemical engineering literature. Harriott (1962), Scriven (1968, 1969), and Sherwood (1974) provide extensive reviews covering transport phenomena across nearly all types of interfaces encountered in engi-

Correspondence concerning this paper should be addressed to John L. Anderson, Department of Chemical Engineering, Carnegie-Mellon University, Pittsburgh, Pennsylvania 15213. Dermot M. Malone is with the Institute of Industrial Research and Standards, Ballymun Road, Dublin 9, Ireland.

neering applications. Membrane transport, in particular, has received considerable attention in recent years because of its importance to such new operations as ultrafiltration, reverse osmosis, and dialysis. The difficulties encountered in analyzing membrane processes usually result from the fact that the boundary-layer resistances at membrane/fluid interfaces represent an appreciable fraction, in some cases the majority, of the total resistance. Generally, a membrane is chosen because of its intrinsic selectivity toward one or more solute species in the bulk fluid; however, a substantial transfer resistance at the fluid/membrane interface essentially negates this selectivity. Thus, quantitative understanding of boundary-layer effects is necessary to permit accurate design of membrane processes.

If one considers the diffusive rate of transfer of a certain solute through a membrane by analogy to an electric current through a passive resistor, then the total resistance R is the sum of the intrinsic membrane resistance (R_m) and the extra membrane boundary-layer contributions (R_∞):

$$R = R_m + 2R_\infty \tag{1}$$

Unless $R_m >> R_\infty$, a reasonably accurate prediction of R_∞ is required to calculate the solute flux across the membrane for a given concentration driving force. Although R_∞ depends on several variables, the most important variable, and the one most easily controlled, is the stirring or convective rate in the bulk fluid (for example, Kaufmann and Leonard, 1968). Unfortunately, most of the research efforts to date have used membranes of poorly understood intrinsic structure, that is, unknown R_m, so that the information gained from such experiments is not as absolute as one might hope.

The measurement of extra membrane transport resistances has been approached in two rather different ways. In the first, one attempts to directly measure by optical techniques concentration profiles at distances very close to the membrane surface (Bollenbeck and Ramirez, 1974; Kapur and MacLeod, 1975; Min et al., 1976). Presently, these optical techniques are restricted to simplified geometries and bulk fluid flow situations where mathematical analysis of the pertinent transport equations is possible. However, as the sophistication of this technique improves, it is anticipated that concentration profiles within a few micrometers of the membrane interface will be measured to allow calculation of transfer coefficients for more complex convective schemes.

In the second approach, an overall (membrane plus boundary layer) mass transfer coefficient is measured, usually as a function of stirring rate of the bulk fluids. The intrinsic membrane resistance is estimated by extrapolation of the data at high stirrer speeds and subtracted from the total resistance at the lower stirrer speeds to give a value for only the boundary-layer resistance. The boundary-layer transfer is characterized by a Sherwood number (N_{Sh}) which is expressed as a simple function of Reynolds (N_{Re}) and Schmidt (N_{Sc}) numbers:

$$N_{Sh} = A(N_{Re})^m(N_{Sc})^{0.33} \tag{2}$$

The Schmidt number dependence is derived from dimensional considerations of the convective-diffusion equation under conditions in which the momentum boundary layer is much larger than the diffusion boundary layer ($N_{Sc} >> 1$). The Sherwood number is proportional to the boundary layer mass transfer coefficient (k_∞) which is defined in terms of the mean flux of solute across the interface (J) and the concentration driving force:

$$k_\infty = \frac{J}{C_\infty - C_i} \tag{3}$$

where C_∞ is the solute concentration far from the membrane and C_i is the concentration at the membrane/bulk fluid interface. Implicitly assumed in the above definition of k_∞ is that the membrane surface is homogeneous with respect to solute diffusion.

Using a rotating disk dialyzer, Litt and Smith (1968) found good agreement between the boundary-layer analysis by Levich (1962) and their experimental data, obtaining $m = 0.5$ and $A = 0.544$ for the parameters in Equation (2) (Levich predicted $A = 0.62$ in the absence of edge effects). In most applications, internal stirring is used to reduce boundary-layer effects because high stirring rates can be achieved and the cell design is simple; however, in this case the parameters A and m must be experimentally determined rather than calculated. Kaufmann and Leonard (1968) measured overall transfer coefficients for the diffusion of various sugars across cellophane membranes in a diaphragm cell with internally mounted, rotating impellers. Although cellophane is generally thought of as a porous membrane, its water fraction is about 70%, and hence the membrane/solution interface is nearly homogeneous in a transport sense. Their data yielded $A = 0.105$ and $m = 0.68$ by least-squares analysis over a range of N_{Re} from 5 000 to 100 000; however, they were forced to rely on extrapolation of a Wilson type of plot to obtain the intrinsic membrane transfer coefficient and hence their results may reflect bias toward the model chosen for extrapolation. Wendt et al. (1971) studied boundary-layer effects in a rotating batch dialyzer, but they too relied on a Wilson extrapolation to deduce intrinsic membrane resistances. Although they observed the Schmidt number dependence given in Equation (2), the value of m was found to equal 1.0; however, the stirring characteristics in this type of cell are surely much different than for a rotating impeller, so that their results cannot be directly compared with those of Kaufmann and Leonard. Smith et al. (1968) and Colton and Smith (1972) reported measurements for the transfer coefficient controlling dissolution of a smooth, stationary disk of benzoic acid into a stirred aqueous phase, thus simulating one-half of a diaphragm diffusion cell. Because the interfacial concentration of benzoic acid could be assumed equal to its equilibrium solubility, direct calculation of the boundary-layer transfer coefficient was possible from material balances on the cell. Their data could be correlated by Equation (2), but a transition in the stirring rate dependence was observed:

$$8\,000 < N_{Re} < 32\,000 \quad m = 0.57,\ A = 0.285 \tag{4}$$

$$32\,000 < N_{Re} < 82\,000 \quad m = 0.75,\ A = 0.0443 \tag{5}$$

The authors interpreted this transition in terms of the laminar-to-turbulent flow transition induced by the rotating impeller. Furthermore, Equation (5) was verified by holding the stirring rate (revolutions per minute) constant and varying the impeller radius.

A mathematical analysis of the convective-diffusion equation near the membrane/solution interface in a diaphragm cell was performed by Colton and Smith (1972) for a circular membrane imbedded in an infinite, otherwise impermeable surface. The flow field generated by the impeller far from the membrane was approximated by a rigid body rotation. For laminar flow conditions, the analysis, when cast into the form of Equation (2), predicted $m = 0.50$, which is in fair agreement with the experimental results shown by Equation (4). The analysis

for turbulent conditions yielded a value of m near 0.75, also in agreement with the experimental results. Their analysis elucidated subtle features of the boundary layer transport process, such as the difference between constant surface concentration and constant surface flux boundary conditions (27% larger k_∞ for the latter condition) and the variability of the local transfer coefficient with position on the membrane surface. The local nature of the transfer coefficient was also examined mathematically by Homsy and Newman (1973) for a fixed disk of constant concentration located beneath a large, rotating disk impeller. Although their analysis predicts that the local Sherwood number increases from a limiting value of 2 at the center of the transfer disk to infinity at the outer edge, the average disk Sherwood number is independent of disk radius.

An alternative approach to modeling boundary-layer effects assumes a turbulent nature for the flow field adjacent to the interface. Such penetration or surface renewal models (Harriott, 1962) are widely used to correlate transfer coefficients for gas/liquid interfaces, although very little application of these models has been made to rigid membrane/fluid interfaces. More recent modifications to this theory were summarized by Scriven (1969). A basic criticism often directed at penetration models is that they contain artificial parameters which, in general, cannot be calculated a priori even if details of the fluid flow field near the interface are known. Petty (1975) has developed a statistical analysis of mass transfer with which the transfer coefficient could be calculated given enough information about the turbulent velocity autocorrelation at the interface; however, no such calculations have been made.

The effect of surface inhomogeneity (that is, transport to a membrane of low porosity) has been treated mathematically by several authors. Kelman (1965) examined a single, circular cylindrical pore of length l and radius r_o which connects two infinite, stagnant reservoirs and obtained

$$\frac{1}{k^{(p)}} \doteq \frac{l}{D_\infty}\left[1+\frac{\pi}{2}\left(\frac{r_o}{l}\right)\right] \tag{6}$$

where the solute transfer coefficient $k^{(p)}$ is based on the pore area. The entrance and exit effects in distorting flux lines each produces an additional equivalent length $\pi r_o/4$ to the diffusion path. Equation (6) can also be obtained from solving Laplace's equation describing steady diffusion from an infinite fluid to a circular pore, which is assumed to have constant concentration over its area, imbedded in an otherwise impermeable wall (Nanis and Kesselman, 1971); if the flux rather than the concentration of solute is assumed constant at the pore mouth, then this additional equivalent length is 8% greater than $\pi r_o/4$ (that is, $8r_o/3\pi$). Prager and Frisch (1975) examined the interaction of equipotential circular sources imbedded randomly in an impermeable wall and found that the resistance per source (or, equivalently, the additional path length per source) is only slightly decreased (<7%) from the single source result for area fractions smaller than 5%.

Keller and Stein (1967) considered the more complex case of steady diffusion through a membrane of parallel, circular pores with large fluid reservoirs on either side. The effect of stirring in these reservoirs was modeled by an unstirred layer of thickness δ (l_1 and l_2 in their nomenclature) adjacent to each face of the membrane; the outer edge of this boundary layer was assumed a plane of constant, uniform concentration. The pores were assigned to a regular array, and their interaction was accounted for by an imaginary cylindrical cell surrounding each pore and extending into the reservoir with zero flux normal to its boundary. In terms of pore length (l), pore radius (r_o), and number of pores per unit area of membrane surface (n), their results can be expressed as

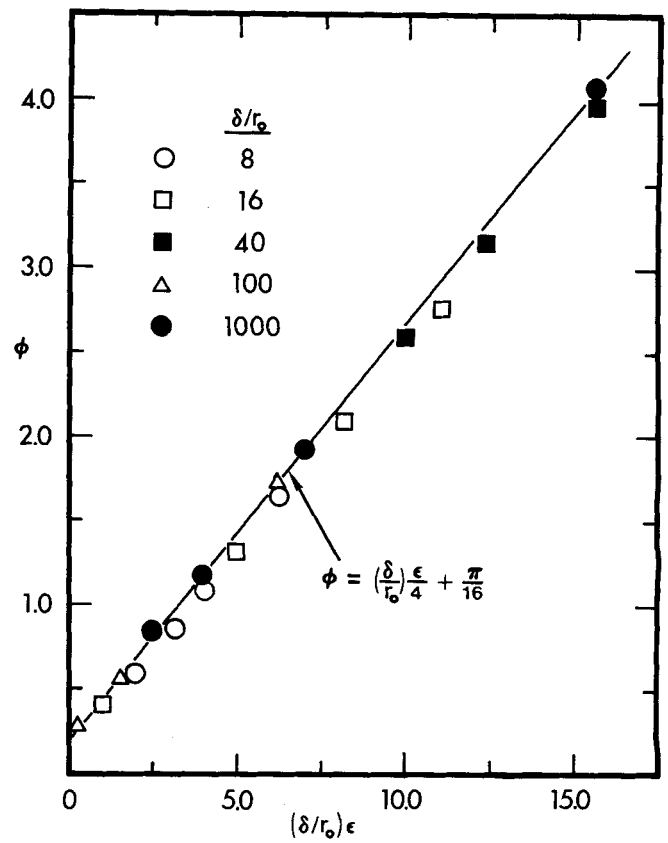

Fig. 1. Parameter ϕ [see Equation (7)] calculated by Keller and Stein (1967). The straight line is Equation (8). ϵ is the membrane porosity $n\pi r_o^2$.

$$\frac{1}{k} = \frac{l}{D_\infty n\pi r_o^2}\left[1+\frac{8r_o}{l}\phi\left(n\pi r_o^2, \frac{\delta}{r_o}\right)\right] \tag{7}$$

where the function ϕ is plotted in their Figure 4 and given analytically in terms of a Bessel function expansion shown in their Equation (9). The overall transfer coefficient k is defined in terms of membrane area and the bulk concentration difference between the well-stirred regions of both reservoirs. Algebraic manipulation suggests that at small pore area fractions and large δ/r_o the function ϕ can be expressed as a function of only the product $(n\pi r_o^2)(\delta/r_o)$. Figure 1 shows that to excellent approximation ϕ is given by

$$\phi \doteq \frac{1}{4}n\pi r_o^2\left(\frac{\delta}{r_o}\right)+\frac{\pi}{16} \tag{8}$$

if $n\pi r_o^2 < 0.5$ and $8 < \delta/r_o < 500$. The first term on the right accounts for the boundary-layer resistance on each side of the membrane, while the second term results from pore entrance and exit effects discussed above. If Equation (8) is substituted into (7), the total resistance ($1/k$) is seen to be the sum of three resistances arranged in series: the pore resistance ($l/D_\infty n\pi r_o^2$), the entrance and exit effects ($\pi r_o/2D_\infty n\pi r_o^2$), and the boundary layer resistance on each side of the membrane ($2\delta/D_\infty$):

$$\frac{1}{k} = \frac{l}{D_\infty n\pi r_o^2}+\frac{\pi r_o/2}{D_\infty n\pi r_o^2}+\frac{2\delta}{D_\infty} \tag{9}$$

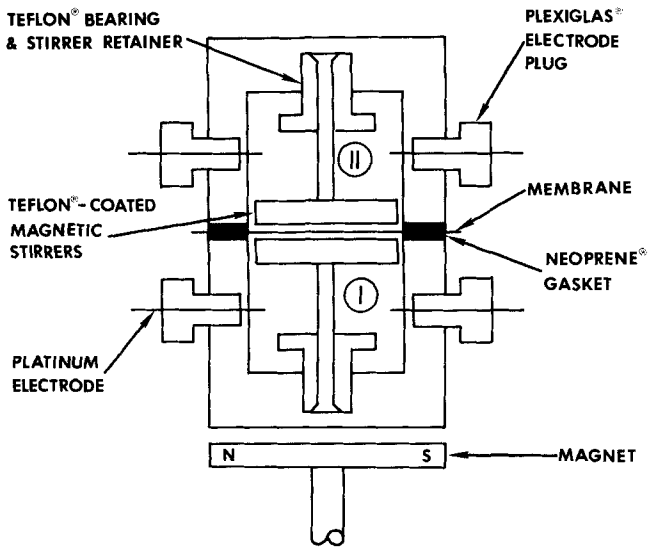

Fig. 2. Diaphragm diffusion cell.

The unstirred layer thickness in Keller and Stein's model is interpreted by us in terms of the boundary-layer mass transfer coefficient:

$$\delta \equiv \frac{D_\infty}{k_\infty} \tag{10}$$

Thus, Equation (2) implies that δ is a function of stirring rate (N_{Re}).

In the experiments described in the next section, k was measured as a function of the number of pores and the stirring rate for potassium chloride diffusion across low porosity (<5%) membranes of nearly identical l and r_o. The membranes were made from mica by the track-etch process; for all membranes, the geometric parameters (n, r_o, l) were determined without the need of any transport experiment. The data were analyzed in accordance with Equation (9), and for each stirrer speed it was found that a single δ could correlate the data. Although the magnitude of δ is not correctly predicted from the correlation proposed by Colton and Smith (1972), the exponential dependence on stirring Reynolds number is the same.

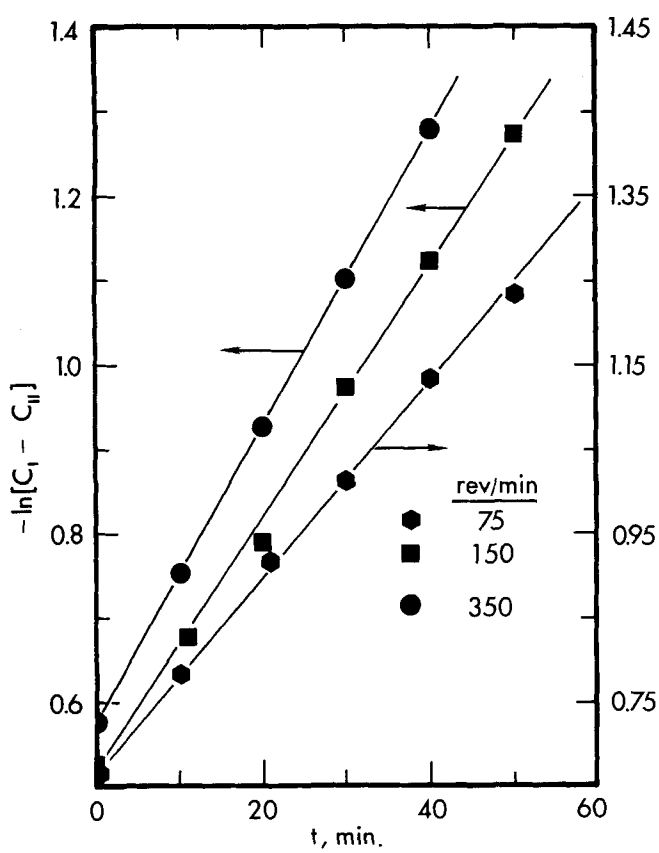

Fig. 3. Data for membrane M375.

EXPERIMENTAL PROCEDURE

The diffusion rates of potassium chloride in aqueous solutions were measured in a diaphragm cell of conventional design (see Figure 2). Salt concentration was measured with a Leeds and Northrup conductivity bridge, and conductivity changes in chambers I and II were monitored as a function of time. Platinized electrode pairs were used in each chamber, and they were routinely calibrated with known concentrations of potassium chloride. Internally seated, nearly cylindrical magnetic stirring bars (Teflon® coated) of length 25 mm and diameter 8 mm were rotated by an external magnet rotated at a speed controlled by a Fisher Dyna SCR motor and controller. The stirring bar was placed about 1 to 2 mm from the face of the membrane. Each chamber had a volume (V) of 0.0114 dm^3 with an internal diameter of 0.28 dm.

With the membrane properly seated between the two chambers, deionized/distilled water was placed in both chambers, and the stirring rate was adjusted to the desired value. At time equal zero, approximately 1 ml of saturated potassium chloride solution was injected quickly (~2 s) into chamber I with a syringe, after which both chambers were sealed to avoid convection and membrane flutter effects. At 5 min intervals, conductivity readings were taken for each chamber, and after about 1 hr the experiment was terminated. The temperature was recorded at each conductivity reading and was found to be nearly constant (± 0.2°C) over the time period of an experiment.

During any one experiment the pseudo steady* instantaneous rate ($\dot{M}$) of potassium chloride transport across the membrane is modeled by

$$\dot{M} = kA_o\,[C_I - C_{II}] \tag{11a}$$

where A_o is the area of membrane over which pores were distributed (that is, pore area $= A_o n\pi r_o^2$; see discussion below on membrane preparation) and k is the overall mass transfer coefficient for the membrane-cell arrangement. A straightforward transient material balance gives

$$\ln\left[\frac{\Delta C(0)}{\Delta C(t)}\right] = \frac{2kA_o t}{V} \tag{11b}$$

$\Delta C(t)$ is the concentration difference between chambers (C_I-C_{II}) at time t. A plot of the left-hand side of (11b) vs. t should yield a straight line, the slope of which can be used to calculate k. Typical data are shown in Figure 3. The overall transfer coefficient was measured as a function of stirrer speed (ω, revolutions per minute) for each membrane, and the results are presented in Table 1.

The most important feature of these experiments is the type of membrane used, that is, track-etched mica (Quinn et al., 1972; Koh and Anderson, 1975). Porous membranes were formed by irradiating a mica disk 55 mm in diameter over a circular target area (A_o) of 200 mm^2 (concentrically located) with fission fragments from a californium 252 source. The tracks created by this irradiation were etched into uniform capillary pores by treatment with aqueous hydrofluoric acid. For any one membrane, all pores were parallel (insured by good collimation during the irradiation process) and had equal radius r_o, defined as the radius of an area-equivalent circle (the pore cross section is actually a 60 deg. rhombus as seen in Figure 4). The number of pores per unit area over the target area was calculated from the irradiation time from a known calibration factor, and the number density was uniform over the

* The pore length was about 5 μm so that diffusional time constants were $\lesssim (5 \times 10^{-4})^2/1.85 \times 10^{-6} = 0.014$ s, much less than the macroscopic (chamber) time constant which was of order 1 hr.

target area of each membrane. The pore radius was determined primarily by the etching rate; however, for each membrane the pore radius was calculated from a transmission electron micrograph similar to the one shown in Figure 4. The pore length determination was made by weighing each membrane before irradiation and using the density of muscovite mica (2.84 kg/dm^3). The end result of this process was a series of membranes each of which was absolutely characterized with respect to structure (n, r_o, l) without the aid of a single transport experiment. Table 2 summarizes the characteristics of the membranes used in our experiments.

RESULTS

The observable effect of stirrer speed on overall mass transfer coefficient is demonstrated in Figure 5 for three membranes of different porosity. Stirring has the greatest effect on the most porous membrane, as one would expect, since the intrinsic resistance is lowest for this membrane. This plot also reminds us that statements to the effect "Boundary phase (unstirred layer) effects were negligible since our stirring speeds were 60 rpm," which are not uncommon in the reporting of dialysis experiments, must be treated with suspicion. In fact, such a statement is obviously in error with regard to the three membranes whose data appear in Figure 5.

Our analysis of the data appearing in Table 1 is based on the model by Keller and Stein (1967) assuming the equivalent boundary-layer thickness δ is a function only of stirrer speed for given placement of the impeller. We start with a simple rearrangement of Equation (9):

$$\frac{(nr_o^2/l)}{k} = \frac{2\delta}{D_\infty}\left[\frac{nr_o^2}{l}\right] + \frac{1}{\pi D_\infty}\left[1 + \frac{\pi r_o}{2l}\right] \quad (12)$$

For each stirrer speed (that is, constant δ), we wish to plot the above in a form from which δ can be deduced by linear regression. This can be accomplished by multiplying Equation (12) by $[1 + \pi r_o/2]^{-1}$. We then scale Equation (12) by reference length l^* and pore radius r^* to obtain

Table 1. Measured Overall Mass Transfer Coefficients

Membrane	Stirrer speed ω, rev · min^{-1}	Mass transfer coefficients* k, 10^{-6} m · s^{-1}	Membrane	Stirrer speed ω, rev · min^{-1}	Mass transfer coefficients* k, 10^{-6} m · s^{-1}
M363	65	1.39	M380	40	0.94
	145	1.55		120	1.02
	250	1.57		220	1.04
	250	1.45		220	1.05
	300	1.55		320	1.06
M376	60	2.34	M382	46	0.95
	145	2.63		120	0.95
	250	2.79		220	0.97
	350	2.83		320	0.97
M371	65	2.57		320	0.99
	250	2.80	M386	40	5.37
	350	3.13		120	7.70
M368	65	3.32		220	8.77
	145	3.95		220	8.79
	250	4.31		320	9.94
	250	4.32	M396	40	3.76
	350	4.52		120	5.71
M375	75†	4.94		191	6.16
	150	7.30		202	6.31
	250	8.49		306	6.65
	250	8.36		320	6.90
	345	8.63	M387	220	9.95

* Corrected to 25°C.

† This datum point was converted to 65 rev/min-equivalent in Figure 6 by assuming $\delta \sim \omega^{-0.57}$, as found by Smith et al. (1968), and using Equation (12). This correction is only 6% in k.

$$\frac{n_r}{k} = \left(\frac{2\delta}{D_\infty}\right) n_r + \frac{l^*}{D_\infty \pi r^{*2}} \quad (13)$$

where the reduced pore number is defined as

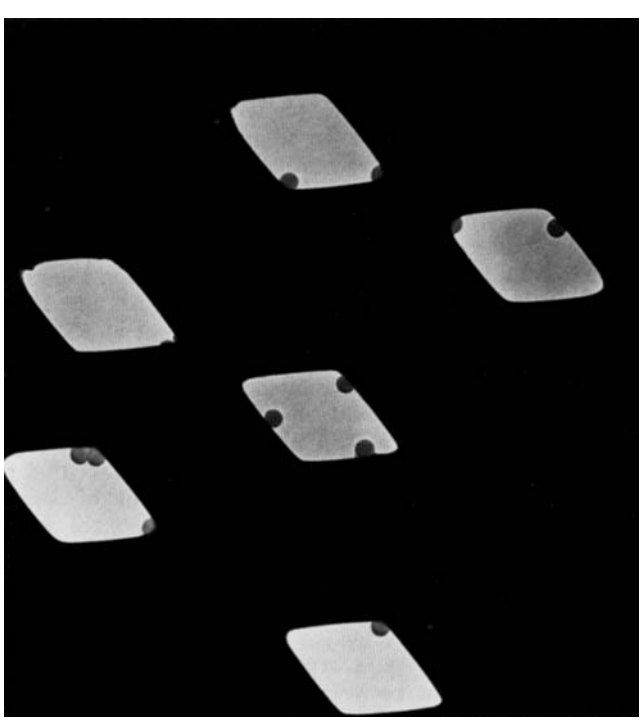

Fig. 4. Transmission electron micrograph of a porous membrane. The spherical objects appearing within the pores are polystyrene latex spheres 0.235 μm in diameter (Dow Chemical Company).

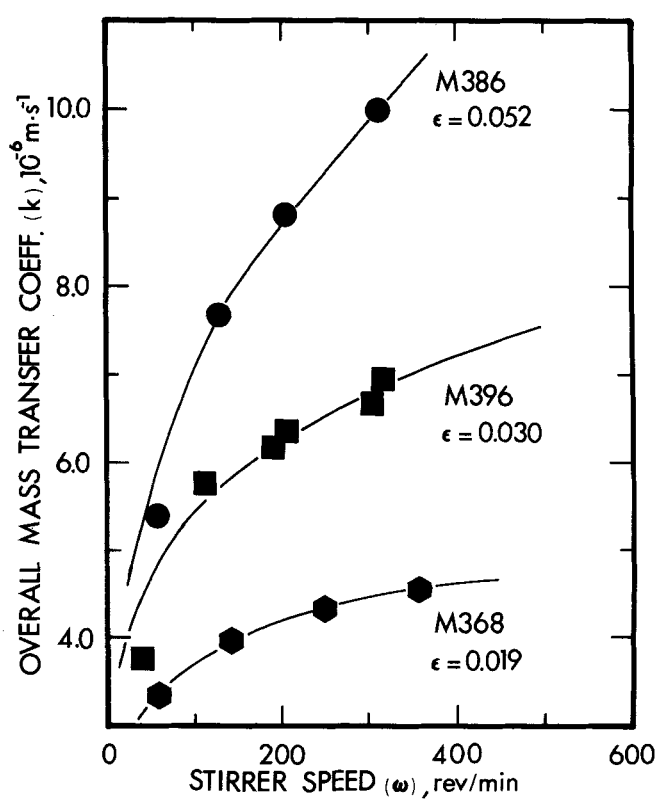

Fig. 5. Effect of stirrer speed on mass transfer coefficient.

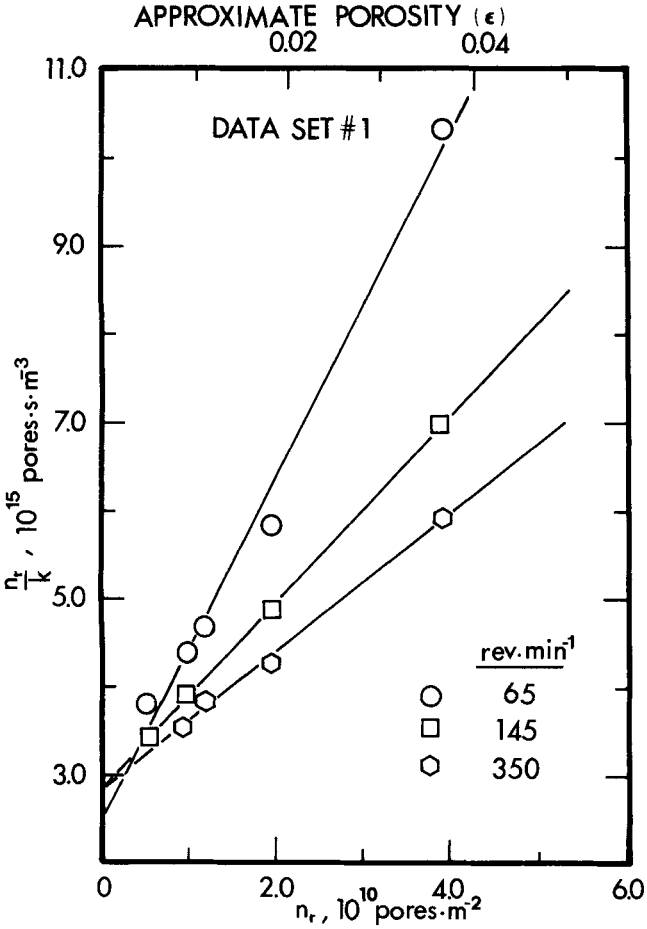

Fig. 6. Resistance per pore vs. number of pores. Data sets No. 1 and No. 2 (Figure 7) differ only in proximity of stirring bar to the membranes (in both cases <2 mm). Data points were calculated from information in Tables 1 and 2 and Equation (14). The straight lines are least-square fits to Equation (13) using all the data shown in Tables 1 and 2.

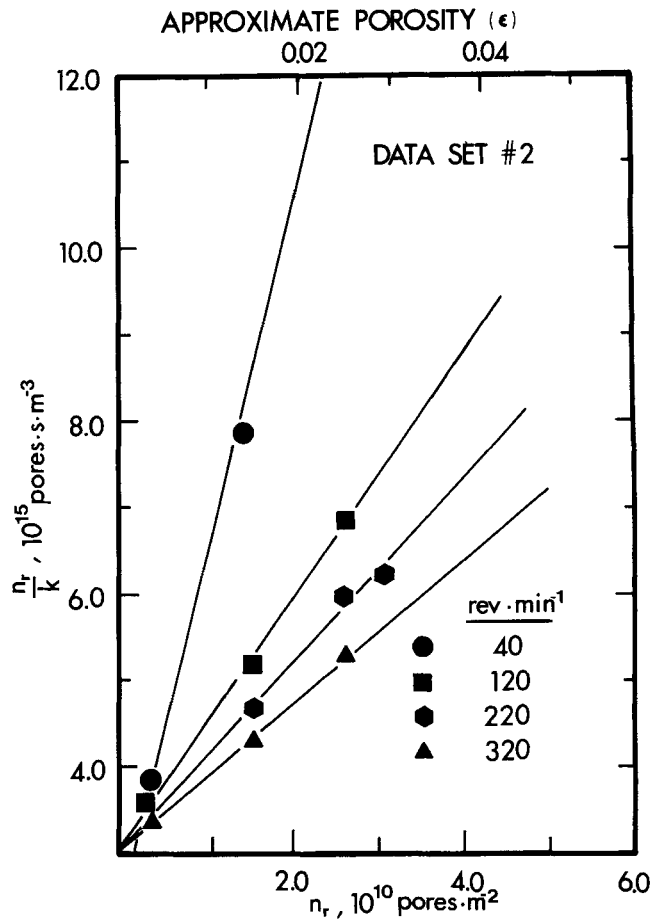

Fig. 7. Resistance per pore vs. number of pores. Another datum point at $\omega = 40$ rev/min and $n_r = 2.62 \times 10^{10}$ is not shown. It falls on the linear regression line drawn for this stirrer speed.

TABLE 2. MEMBRANE CHARACTERISTICS

Membrane	Pore length (l, μm)	Pore radius (r_o, μm)*	Pore density (n, 10^9 pores · m^{-2})	Porosity (ϵ)†
M363	5.10	0.57	4.97	0.005
M376	5.00	0.55	9.94	0.010
M371	5.10	0.50	14.08	0.011
M368	5.26	0.59	17.40	0.019
M375	5.40	0.56	51.34	0.050
M380	4.87	0.48	4.42	0.0032
M382	5.48	0 49	4.42	0.0034
M386	5.22	0.71	33.0	0.052
M387	4.78	0.71	35.8	0.057
M396	5.45	0.65	22.3	0.030

* Determined by transmission electron microscopy.
† $\epsilon = n\pi r_o^2$.

$$n_r \equiv n\left(\frac{l^*}{l}\right)\left(\frac{r_o}{r^*}\right)^2\left[1+\frac{\pi r_o}{2l}\right]^{-1} \qquad (14)$$

The quantity n_r/k can be considered a resistance per pore; that is, if over a unit area of membrane there are n_r pores in parallel, each of resistance n_r/k, then the total diffusional resistance of that area of membrane is $1/k$. Since l^*, r^*, and D_x are constants, the validity of Equation (13), or equivalently Equation (9), can be tested by plotting n_r/k vs. n_r for a constant stirrer speed. This plot should be a straight line of slope $(2\delta/D_\infty)$ from which δ can be computed. The data plotted in Figures 6 and 7 were obtained from the data in Tables 1 and 2 and Equation (14). To avoid undue congestion, not all the data in these tables are plotted for $n_r < 2 \times 10^{10}$. The linearity of these graphs demonstrates that Equation (9) is an accurate representation for low porosity membranes. The straight lines drawn in these two figures are least-squares fits to Equation (13), using all the data of Tables 1 and 2. The slopes of these lines were used to compute the δ values which are shown in Figure 8.

Our reference dimensions were $r^* = 0.51$ and $l^* = 5.0$ μm, and the integral diffusion coefficient at 25°C for potassium chloride is 1.85×10^{-9} m^2/s (Mills and Woolf, 1968). Hence, the intercept for all straight lines in Figures 6 and 7 should be 3.31×10^{15} s/m^3, while the actual intercepts are all about 3.0×10^{15} or 10% too low. This discrepancy may be due to the fact that r^* actually represents an absolute measurement of length under the electron microscope, and a 5% error in its determination would account for this 10% error. Furthermore, our entrance and exit corrections [$\pi r_o/2l$ term in Equation (14)] may be in error, since our pores were not circular.

A log plot of δ vs. stirrer speed (Figure 8) shows excellent agreement between the two sets of data. Since the only difference between these two sets of experiments was placement of the impeller, we agree with the conclusion of Smith et al. (1968) that the gap between impeller and membrane is not crucial if it is small, in

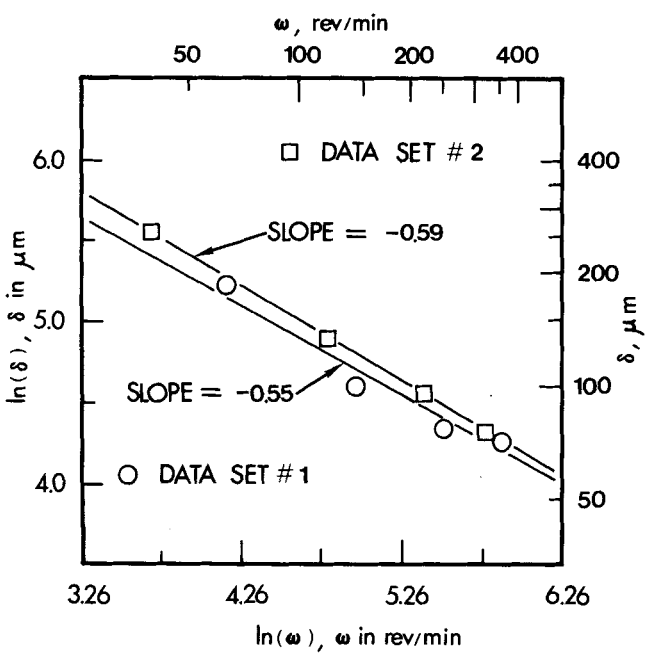

Fig. 8. Stirrer speed dependence of equivalent boundary-layer thickness (δ). The δ values were computed from the slopes of the regression lines in Figures 6 and 7 and from Equation (13).

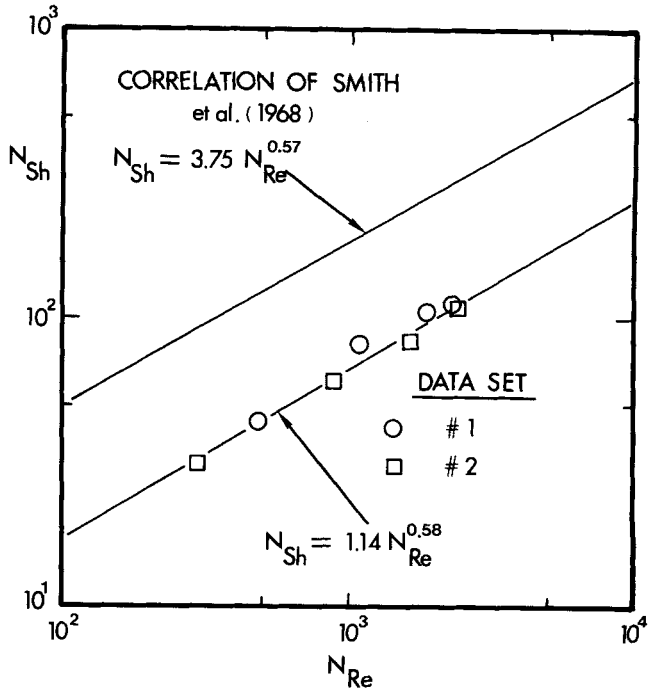

Fig. 9. Comparison of present data with literature correlation. Sherwood numbers were calculated fom the data in Figure 8 using Equation (10).

our case <2 mm. Each datum set exhibits a linear relationship with the slopes equalling −0.59 and −0.55. Since δ is related to k_∞ by Equation (10), these slopes are in excellent agreement with the dissolution data of Smith et al. [$m = 0.57$ in Equation (2)].

Smith et al. (1968) propose correction factors which can be used to adjust their experimentally determined parameter A in Equation (2) for use in other cells of similar geometry:

$$N_{Sh} = (\Phi\Psi)An_{Re}^{0.57}N_{Sc}^{0.33} \qquad (15)$$

The factor Φ (see Figure 11 of their paper) accounts for relative membrane permeability and should equal about 1.2 for our membranes (typical porosity ~0.03). The factor Ψ corrects for the ratio of (active)* membrane radius/impeller radius if different from their experimental value of 1.1. Our ratio was 0.64 (=8.0/12.5), and extrapolation of the curve in Figure 9 of their paper yields $\Psi \approx 1.4$. Using their experimental value of $A = 0.285$ and $N_{Sc} = 480$, Smith et al. would predict our boundary-layer Sherwood number to be given by

$$N_{Sh} = (3.75)N_{Re}^{0.57} \qquad (16)$$

The above equation is plotted along with our data ($N_{Sh} = a/\delta$) in Figure 9. Although the stirring rate dependence is as predicted, the magnitudes of our experimental points are considerably lower than predicted by Equation (16). A least-squares fit through our data yields

$$N_{Sh} = (1.14)N_{Re}^{0.58} \qquad (17)$$

indicating that the prediction of Smith et al. is about a factor of 3 too high for our system.

The discrepancy between the measured boundary-layer mass transfer coefficients and those predicted by Equation (16) suggests that the details of the transport phenomena near low porosity membranes are significantly different than near a smooth, homogeneous surface such as benzoic acid. Since Smith et al. (1968) successfully correlate the data of Kaufmann and Leonard (1968) using Equation (15), we further suggest that boundary conditions differ between high porosity (≈ homogeneous) and low porosity membranes. However, it must be noted that the factor of 3 difference between Equations (16) and (17) could partially be the result of differences in cell and impeller geometry. For example, Smith et al. used a four-blade impeller (as did Kaufmann and Leonard), whereas our impeller was a cylindrical bar. Also, our impeller was a half length (b) larger than the radius of the active membrane area (12.5 vs. 8.0 mm), rather than the reverse which existed in the diaphragm cell studied by Smith et al.; thus, cell wall effects could have been very different in their experiments compared to ours. In any case, we conclude that the predictive correlations proposed by Colton and Smith (1972) show the proper stirring rate dependence but cannot be relied upon to give an accurate estimate of the boundary-layer mass transfer coefficient for a low porosity membrane such as studied here.

In summary, our results show that the stagnant film model, or, more precisely, the linear addition of boundary-layer and intrinsic membrane resistances proposed by Equation (9), provides an excellent quantitative description for diffusion across membranes of low porosity. The film thickness appears to be only a function of stirrer speed, and perhaps cell and stirrer geometry, but independent of membrane permeability at the low porosities examined. After equivalent film thicknesses are converted to boundary-layer transfer coefficients, the resulting Sherwood number-Reynolds number correlation yields an exponent equal to the value determined for homogeneous surfaces, although the magnitude of the Sherwood number appears to be lower for low porosity membranes. From the data of our experiments alone, we cannot distinguish how much of this discrepancy can be attributed to cell design and how much to a fundamental difference in the transport phenomena occurring at heterogeneous vs. homogeneous membrane/fluid interfaces.

* In our case, the active radius equaled the radius of the target area A_o.

ACKNOWLEDGMENT

We thank Mr. Roger LeBrun, Mr. Richard Weissman, and Professor George Cocks for their invaluable assistance in characterizing the mica membranes by electron microscopy. Also appreciated is the help given to us by Mr. Daniel Teichman in gathering data for salt diffusion across membranes. We acknowledge the partial support of this project by NSF Grant ENG 73-04112 A01. Finally, we appreciate the very helpful comments by the reviewers.

NOTATION

A = prefactor in Equation (2)
a = radius of target area, mm
A_0 = target area of irradiated membrane; its value was 200 mm^2
b = half length of stirring bar, mm
C_∞ = concentration of solute in bulk solution, kg·dm^{-3}
C_i = concentration of solute at the membrane/solution interface, kg·dm^{-3}
C_I = concentration of solute in chamber I of diaphragm diffusion cell, kg·dm^{-3}
C_{II} = concentration of solute in chamber II of diaphragm diffusion cell, kg·dm^{-3}
$\Delta C(t) = C_I - C_{II}$ at time t
D_∞ = integral averaged diffusion coefficient of potassium chloride m^2·s^{-1}
J = diffusive flux of solute across the membrane, kg·m^{-2}·s^{-1}
k = overall membrane mass transfer coefficient for a membrane, defined by Equation (11a), m·s^{-1}
k_∞ = boundary-layer mass transfer coefficient defined by Equation (3), m·s^{-1}
$k^{(p)}$ = mass transfer coefficient for a single pore in a membrane, m·s^{-1}
l = membrane thickness, μm
l^* = reference membrane thickness introduced in Equation (13), μm
M = total rate of mass transfer across a membrane from chamber I to chamber II, kg·s^{-1}
m = exponent for N_{Re} arising in Equation (2)
n = pore density of membrane, pores·m^{-2}
n_r = reduced pore density defined in Equation (14), pores·m^{-2}
$N_{Sh} = k_\infty a/D_\infty$ = Sherwood number
$N_{Re} = \omega a^2/\nu$ = Reynolds number
$N_{Sc} = \nu/D_\infty$ = Schmidt number
R = overall membrane mass transfer resistance, s·m^{-1}
r^* = reference pore radius introduced in Equation (13), μm
R_m = mass transfer resistance of membrane, s·m^{-1}
r_o = radius of circle of equal area to rhomboidal pore, μm
R_∞ = boundary-layer mass transfer resistance, s·m^{-1}
t = time, s
V = chamber volume of diaphragm diffusion cell, dm^3

Greek Letters

δ = boundary-layer thickness, μm
$\epsilon = n\pi r_o^2$ = membrane porosity
ν = kinematic viscosity, m^2·s^{-1}
ϕ = function used by Keller and Stein (1967) [see Equation (7)]
Φ, Ψ = correction factors for membrane permeability and stirrer/membrane size, used by Smith et al. (1968) to modify A of Equation (2) [see Equation (15)]
ω = stirrer speed, rad·s^{-1} or rev·min^{-1}

LITERATURE CITED

Bollenbeck, P. H., and W. F. Ramirez, "Use of a Rayleigh Interferometer for Membrane Transport Studies," *Ind. Eng. Chem. Fundamentals*, **13**, 385 (1974).
Colton, C. K., and K. A. Smith, "Mass Transfer to a Rotating Fluid: Part II. Transport from the Base of an Agitated Cylindrical Tank," *AIChE J.*, **18**, 958 (1972).
Harriott, P., "A Review of Mass Transfer to Interfaces," *Can. J. Chem. Eng.*, **40**, 60 (1962).
Homsy, R. V., and J. Newman, "Mass Transfer to a Plane Below a Rotating Disk at High Schmidt Numbers," *AIChE J.*, **19**, 929 (1973).
Kapur, D. N., and N. Macleod, "Holographic Determination of Local Mass Transfer Coefficients at a Solid-Liquid Boundary," *ibid.*, **21**, 184 (1975).
Kaufmann, T. G., and E. F. Leonard, "Mechanism of Interfacial Mass Transfer in Membrane Transport," *ibid.*, **14**, 421 (1968).
Keller, K. H., and T. R. Stein, "A Two-Dimensional Analysis of Porous Membrane Transport," *Math. Biosciences*, **1**, 421 (1967).
Kelman, R. B., "Steady-State Diffusion Through a Finite Pore into an Infinite Reservoir: An Exact Solution," *Bull. Math. Biophys.*, **27**, 57 (1965).
Koh, W-H., and J. L. Anderson, "Electroosmosis and Electrolyte Conductance in Charged Microcapillaries," *AIChE J.*, **21**, 1176 (1975).
Levich, V. G., *Physicochemical Hydrodynamics*, Prentice-Hall, Englewood Cliffs, N. J. (1962).
Litt, M., and W. G. Smith, "Artificial Membranes: A New Type of Cell for Measuring Diffusional Resistance," *Science*, **160**, 201 (1968).
Mills, R., and L. A. Woolf, "The Diaphragm Cell," Diffusion Research Unit, Research School of Physical Sciences, Australian National University, Canberra, A.C.T. Australia (1968).
Min, S., J. L. Duda, R. H. Notter, and J. S. Vrentas, "An Interferometric Technique for the Study of Steady State Membrane Transport," *AIChE J.*, **22**, 175 (1976).
Nanis L., and W. Kesselman, "Engineering Applications of Current and Potential Distributions in Disk Electrode Systems," *J. Electrochem. Soc.: Electrochemical Science*, **118**, 454 (1971).
Petty, C. A., "A Statistical Theory for Mass Transfer Near Interfaces," *Chem. Eng. Sci.*, **30**, 413 (1975).
Prager, S., and H. L. Frisch, "Interaction Between Penetration Sites in Diffusion Through Thin Membranes," *J. Chem. Phys.*, **62**, 89 (1975).
Quinn, J. A., J. L. Anderson, W. S. Ho, and W. J. Petzny, "Model Pores of Molecular Dimension—The Preparation and Characterization of Track-Etched Membranes," *Biophys. J.*, **12**, 990 (1972).
Scriven, L. E., "Flow and Transfer at Fluid Interfaces," *Chem. Eng. Ed.*, 150 (Fall, 1968); 26 (Winter, 1969); 94 (Spring, 1969).
Sherwood, T. K., "The Development of Mass Transfer Theory," *ibid.*, 204 (Fall, 1974).
Smith, K. A., C. K. Colton, E. W. Merrill, and L. B. Evans, "Convective Transport in a Batch Dialyzer: Determination of True Membrane Permeability From a Single Measurement," *Chem. Eng. Progr Symposium Ser. No. 84*, **64**, 45 (1968).
Wendt, R. P., R. J. Toups, J. K. Smith, N. Leger, and E. Klein, "Measurements of Membrane Permeabilities Using a Rotating Batch Dialyzer," *Ind. Eng. Chem. Fundamentals*, **10**, 406 (1971).

Manuscript received August 9, 1976; revision received November 29, and accepted December 9, 1976.